Available online at www.sciencedirect.com
ScienceDirect
European Journal of Pharmaceutics and Biopharmaceutics 68 (2008) 526–534
European Journal of Pharmaceutics and Biopharmaceutics
www.elsevier.com/locate/ejpb

Research paper

Nasal absorption enhancement of insulin using PEG-grafted chitosan nanoparticles

Xinge Zhang [a], Huijie Zhang [a], Zhongming Wu [b], Zhen Wang [a], Haimei Niu [a], Chaoxing Li [a,*]

[a] *The Key Laboratory of Functional Polymer Materials of Ministry Education, Institute of Polymer Chemistry, Nankai University, Tianjin, China*
[b] *Metabolic Diseases Hospital, Tianjin Medical University, Tianjin, China*

Received 22 January 2007; accepted in revised form 10 August 2007
Available online 16 August 2007

Abstract

The objective of this work was to explore the potential of polyethylene glycol-grafted chitosan (PEG-*g*-chitosan) nanoparticles as a system for improving the systemic absorption of insulin following nasal administration. Insulin-loaded PEG-*g*-chitosan nanoparticles were prepared by the ionotropic gelation of PEG-*g*-chitosan solution using tripolyphosphate ions as the crosslinking agent. The nanoparticles were in the size range 150–300 nm, had a positive electrical charge (+16 to +30 mV) and were associated with insulin (loading efficiency 20–39%). The physicochemical properties of nanoparticles were affected by the composition of the copolymer. *In vitro* insulin release studies showed an initial burst followed by a slow release of insulin. Intranasal administration of PEG-*g*-chitosan nanoparticles in rabbits enhanced the absorption of insulin by the nasal mucosa to a greater extent than a suspension of insulin-PEG-*g*-chitosan and control insulin solution. PEG-*g*-chitosan nanoparticles are promising vehicles for insulin transport through the nasal mucosa.

Keywords: PEG-*g*-chitosan; Nanoparticles; Nasal delivery; Insulin; Blood glucose; Absorption enhancement

1. Introduction

Oral delivery offers a comfortable and physiologically acceptable way to administer a wide range of drugs. However, macromolecular drugs such as peptides and proteins cannot be given orally because they are degraded by the proteolytic enzymes in the stomach, and most of these drugs need to be administered repeatedly by injection. Significant efforts have been made to explore alternative routes for drug administration. Intranasal drug delivery is a convenient and reliable method that has many advantages, such as a large absorptive surface area and high vascularity of the nasal mucosa, where drugs absorbed from the nasal cavity pass directly into the systemic circulation, thereby avoiding first-pass liver metabolism [1]. However, the administration of macromolecules by this route is hampered by the chemical and physical instability of these molecules, and by the high metabolic activity and limited permeability of the mucosal barriers [2].

There are many approaches to improving the absorption of peptides and proteins through the nasal mucosa by the use of absorption enhancers, enzyme inhibitors and solutions of bioadhesive polymers or bioadhesive microspheres [3–5]. The use of most absorption enhancers, such as surfactants, bile salts and fatty acids, is accompanied by mucosal damage [6]. However, the absorption-enhancing effect of the polysaccharide chitosan outweighs the damage caused to the nasal mucosa [7]. The mechanism of action of chitosan is suggested to be a combination of bioadhesion and a transient widening of the tight junctions between epithelial cells [8]. It should be noted that chitosan adsorbs plasma proteins in contact with blood, which leads to

* Corresponding author. The Key Laboratory of Functional Polymer Materials of Ministry Education, Institute of Polymer Chemistry, Nankai University, Tianjin 300071, China. Tel.: +86 22 23501645; fax: +86 22 23505598.
E-mail address: lcx@nankai.edu.cn (C. Li).

0939-6411/$ - see front matter © 2007 Elsevier B.V. All rights reserved.
doi:10.1016/j.ejpb.2007.08.009

surface-induced thrombosis occurring at the blood-biomaterial interface [9].

PEG-*g*-chitosan copolymers have been synthesized in an attempt to increase the solubility and improve the biocompatibility of chitosan [10]. Moreover, modification of chitosan with PEG can resist adsorption of plasma proteins in contact with blood through the steric repulsion mechanism [9]. Insulin-PEG-*g*-chitosan nanocomplexes are formed by intermolecular hydrogen bonding in an aqueous solution [11]. On the basis of these results, we decided to explore the potential of PEG-*g*-chitosan nanoparticles as a delivery vehicle for nasal administration of proteins and peptides.

The goal of the present work was to associate insulin, as a model peptide, with PEG-*g*-chitosan nanoparticles. We first studied the preparation of insulin-loaded nanoparticles by using different formulation conditions and characterized their physicochemical properties and the *in vitro* release of insulin. Then, the ability to enhance the nasal absorption of insulin was investigated by determining the decrease in plasma glucose levels following nasal administration. Finally, we studied the effect of the composition of PEG-*g*-chitosan on the ability of the nanoparticles to transport insulin across the nasal mucosa in rabbits.

2. Materials and methods

2.1. Materials

Chitosan (degree of deacetylation 90%; with molecular mass of 6 and 20 kDa) was obtained from the Zhejiang Yuhuan Ocean Biochemical Co., Ltd. (Zhejiang, China). PEG350 (350 Da) and PEG750 (750 Da) were purchased from the Aldrich Chemical Co., Inc. (USA). Pure crystalline porcine insulin (with a nominal activity of 28 IU/mg) that was used without further purification was obtained from the Xuzhou Wanbang Biochemical Co., Ltd. (Jiangsu, China). All other chemicals were of analytical grade.

2.2. Synthesis of PEG-g-chitosan

PEG-*g*-chitosan was prepared as described by Harris et al. [12]. First, PEG-aldehyde was prepared by oxidation of PEG with DMSO/acetic anhydride. Acetic anhydride was added to the mixture under nitrogen after MeO-PEG was dissolved in anhydrous DMSO/chloroform (9:1, v/v) with acetic anhydride/PEG molar ratio of 12, and the mixture was stirred for 9 h at room temperature under nitrogen. The reaction mixture was neutralized with 1 M NaOH and used directly for the next reaction.

PEG-*g*-chitosan was prepared by alkylation of chitosan followed by Schiff base formation. PEG-aldehyde with different molar ratios to the amino groups of chitosan was added to a mixture of acetic acid and methanol (2:1, v/v), and the mixture was stirred for 30 min at room temperature. A solution of sodium tetrahydroborate ($NaBH_4$) was added slowly to the reactant mixture at pH 6.5 with vigorous stirring at a constant molar ratio of 10:1 for $NaBH_4$/PEG-aldehyde. The resultant mixture was dialyzed (3500 Da cutoff) first against 0.05 M NaOH and then distilled water before the solution was freeze-dried. PEG-*g*-chitosan was finally obtained by removal of unreacted PEG with excess acetone.

2.3. Preparation of PEG-g-chitosan nanoparticles

The preparation of PEG-*g*-chitosan nanoparticles based on the ionic gelation of chitosan with tripolyphosphate anions (TPP) was adapted from the method described by Calvo et al. [13]. Experiments were done to identify the production zone for formation of nanoparticles. For this purpose, PEG-*g*-chitosan was dissolved in (2%, w/v) acetic acid at various concentrations of PEG-*g*-chitosan (0.5, 1.0, 1.5, 2.0, 2.5, 3.0, 4.0, 5.0, 7.0, and 9.0 mg/ml). TPP was dissolved in purified water at the same concentrations as PEG-*g*-chitosan. Finally, various volumes of TPP solution (0.5, 1.0, 2.0, and 3 ml) were added dropwise to 5 ml of PEG-*g*-chitosan solution with stirring at room temperature. The samples were analyzed visually and three different systems were identified: clear solution, opalescent suspension (nanoparticles) and aggregates. The opalescent suspension, which should correspond to a suspension of very small particles, was investigated further by adding 2 ml of TPP solution to 5 ml of PEG-*g*-chitosan solution, thus achieving a final concentration of PEG-*g*-chitosan between 0.38 and 2.86 mg/ml and a final concentration of TPP between 0.28 and 1.14 mg/ml. The appearance of these preparations was observed microscopically and samples were classified as aggregates or nanoparticles, as shown in Fig. 1. To evaluate the effect of PEG-*g*-chitosan on the nasal absorption of insulin, further experiments were conducted using a PEG-*g*-chitosan final concentration of

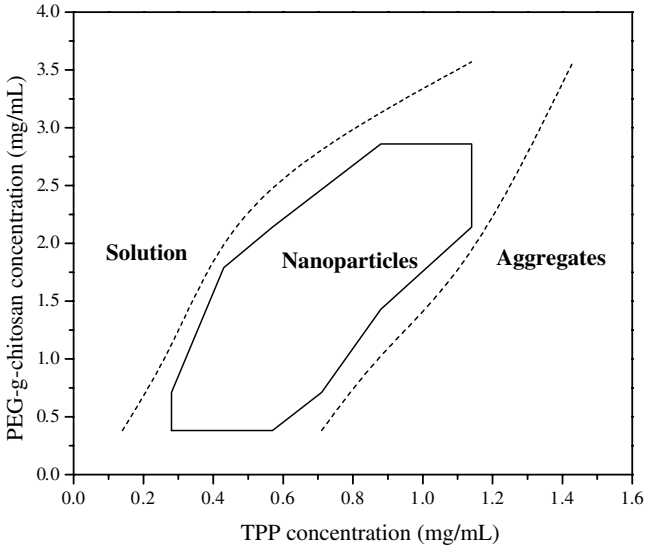

Fig. 1. Identification of PEG-*g*-chitosan and TPP concentrations for the formation of nanoparticles.

1.79 mg/ml and a final concentration of TPP of 0.11 mg/ml; thus, the PEG-*g*-chitosan/TPP ratio was 4.2:1 (w/w).

The following method was used for the preparation of PEG-*g*-chitosan nanoparticles by intermolecular hydrogen bonding in an aqueous solution as reported by Ohya et al. [11]. A 1.78 mg/ml solution of PEG-*g*-chitosan swollen in PBS was stirred for 10 min to give a milky suspension, which was sonicated at room temperature using a probe-type sonicator for 4 min. The PEG-*g*-chitosan suspension obtained was incubated at room temperature for 1 day before measurement.

2.4. Preparation of insulin-loaded nanoparticles

Insulin-loaded nanoparticles were formed spontaneously upon incorporation of 2 ml of 1.5 mg/ml TPP solution containing various concentrations of insulin (0.5, 1.0, and 2.0 mg/ml) to 5 ml of 2.5 mg/ml PEG-*g*-chitosan acidic solution with stirring by a magnetic follower.

2.5. Characterization of nanoparticles

The morphological examination of nanoparticles was performed by transmission electron microscopy (TEM) (Philips EM400ST). Samples were placed on copper grids with Formvar films for viewing under the microscope. Particle size and zeta potential were determined by photo-correlation spectroscopy (PCS, BI-200SM) and laser Doppler anemometry (Zetasizer 3000HS), respectively. For the determination of the electrophoretic mobility, the samples were placed in electrophoretic cells where a potential of ±150 mV was established. The zeta potential was the average value of analysis in triplicate.

The surface chemical composition of nanoparticles was analyzed by X-ray photoelectron spectroscopy (XPS) with a Perkin-Elmer PHI 1600 spectrometer using a Mg Kα X-ray source. All binding energies (BEs) were referenced to the C1s hydrocarbon peak at 284.8 eV.

2.6. Evaluation of the insulin-loading capacity of nanoparticles

The association efficiency of insulin was determined upon separation of nanoparticles from the aqueous medium containing free insulin by centrifugation (16,000 rpm, 30 min, 15 °C). The amount of free insulin in the supernatant was measured by the Bradford method using a UV spectrometer (Shimadzu UV-2550) at 595 nm [14]. The insulin loading capacity (LC) and the association efficiency (AE) were calculated as follows:

$$\mathrm{AE} = \frac{\text{total insulin} - \text{free insulin}}{\text{total insulin}} \times 100$$

$$\mathrm{LC} = \frac{\text{total insulin} - \text{free insulin}}{\text{nanoparticles weight}} \times 100$$

All measurements were performed in triplicate and averaged.

2.7. In vitro release studies

Insulin release was determined by incubating nanoparticles at 37(±0.5) °C in 2 ml of phosphate buffer (pH 7.4) with horizontal shaking. At predetermined time-points, samples were centrifuged and then the supernatant was taken and replenished by fresh buffer solution. The amount of free insulin was determined by the Bradford method, and a calibration curve was made using non-loaded nanoparticles to correct for the intrinsic absorption of the polymer. In each experiment, the samples were analyzed in triplicate and the error bars in the plot were the standard deviation.

2.8. In vivo studies

The nasal absorption study was done with female New Zealand rabbits (2–3 kg, 3 months old) provided by the animal center of the Affiliated Hospital of Shandong University of Traditional Chinese Medicine. Before the experiments, all animals were fasted overnight (18 h) with free access to drinking water. In order to avoid any influence of anesthesia, animals remained conscious during the experiments [15,16].

A suspension of insulin-PE3gC24 (PE3gC24, 0.5 mg/kg), four types of insulin-loaded PEG-*g*-chitosan nanoparticles, and a solution of insulin as the control; were administered intranasally via ~3 cm of polyethylene tubing (~2 mm diameter). The insulin formulations (5 IU/kg body weight) were administered in a volume range of 200–250 μl, depending on insulin loading capacity and animal weight. The dose of nanoparticles administered varied between 0.61 and 0.81 mg/kg and dose was divided equally between the two nostrils to maximize the nasal mucosal surface area exposed to the drug.

Blood samples (2.0 ml) were taken from an ear vein 15 min before drug administration to establish baseline levels, and after drug administration at predetermined time-points (15, 30, 60, 90, 120, 180, 240, and 300 min). The blood samples were centrifuged at 10,000 rpm for 5 min to obtain serums. The plasma glucose concentration was determined with a blood glucose assay kit using the glucose oxidase method. Serum insulin levels were determined with radioimmunoassay.

2.9. Statistical analysis of in vivo data

The plasma glucose concentration of each rabbit before administration was taken as the baseline level, and the changes in plasma glucose concentrations (percentage of baseline level) at different time points after administration were calculated and plotted vs. time. The area under the curve (AUC) for plasma insulin vs. time was calculated with the trapezoidal method. Data from different experimental groups were compared with the corresponding control group (insulin control solution) by ANOVA with Bonferroni adjustment and the level of statistical significance was set at $p < 0.05$.

3. Results and discussion

3.1. Synthesis of PEG-g-chitosan

The synthesis of PEG-*g*-chitosan has been reported by Harris et al. [12]. Chitosan was modified with a PEG-aldehyde to yield an imine (Schiff base) and subsequently PEG-*g*-chitosan was produced through reduction with $NaBH_4$ (Fig. 2). The final purified product of PEG-*g*-chitosan was analyzed by ^1H NMR. The H-1 proton signal from chitosan was observed at 4.9 ppm, and that of the methyl group of PEG was observed at 3.4 ppm. The degree of PEG substitution (DS) was evaluated by elemental analysis (Table 1). By changing the molar ratio of PEG-aldehyde to the amino groups of chitosan, samples with different graft weight ratios (wt%) were obtained (Table 1). We used the following abbreviated nomenclature for the copolymers: PEmgCnX, where PEm denotes the molecular mass of PEG in Da, Cn represents the molecular mass of chitosan and X shows the molar ratio of PEG/chitosan.

The data shown in Table 1 indicate that DS depended on the molar ratio of PEG-aldehyde to amino group of chitosan, but was influenced by PEG molecular mass. DS decreased with increasing PEG molecular mass. The excess PEG-aldehyde over the amino groups of chitosan will give high DS, but this might cause the loss of the chemical properties of chitosan. Therefore, water-soluble PEG-*g*-chitosan was obtained by grafting an appropriate amount of PEG onto the chitosan backbone, which was used as the drug delivery material. Furthermore, copolymers were prepared with chitosan 6 kDa (with almost same wt% as that of chitosan 20 kDa) in the same manner (Table 1). However, all of the samples had a low DS value, possibly because the excess of $NaBH_4$ made the reaction solution more basic and the solubility of chitosan less, hindering its chemical reaction with PEG. On the other hand, the steric hindrance of the association of PEG with the chitosan backbone might prevent further reaction between chitosan and free PEG.

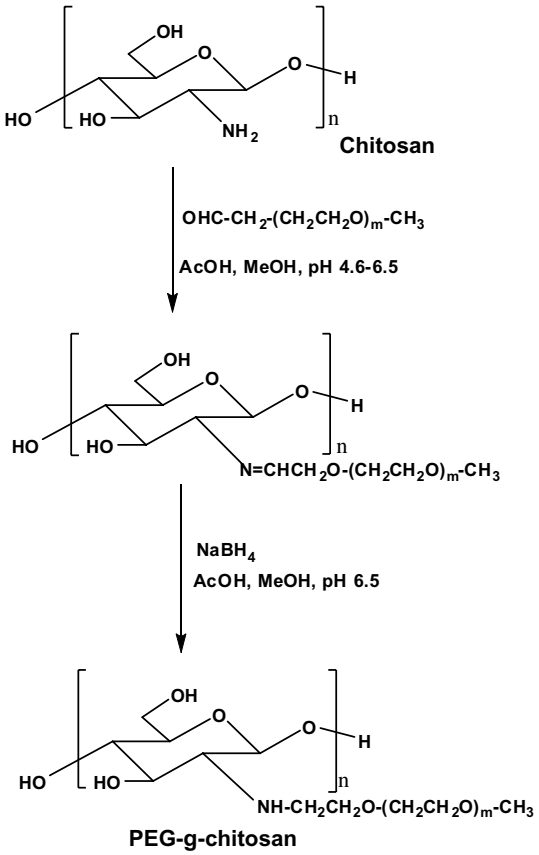

Fig. 2. The synthesis of PEG-*g*-chitosan.

3.2. Conditions for the formation of PEG-g-chitosan nanoparticles

In order to investigate the feasibility of preparing PEG-*g*-chitosan nanoparticles by the ionotropic gelation method, we adopted a protocol similar to that established for the development of chitosan nanoparticles by ionic gelation with TPP [13]. The final concentration of PEG-*g*-chitosan can be up to 2.86 mg/ml while the maximum TPP concentration is 1.14 mg/ml. Due to the presence of PEG, a higher concentration of TPP was needed for the preparation of PEG-*g*-chitosan compared to that used for the preparation of chitosan nanoparticles by Calvo et al.

The shape of nanoparticles was examined by TEM. Fig. 3 shows PEG-*g*-chitosan nanoparticles with a compact core surrounded by a fluffy coat made of PEG, which was verified by XPS analysis (see Table 2). The C1s and O1s binding energies do not permit the identification of PEG, since both chitosan and PEG have the same functional groups (C–C, C–H and C–O). However, the ratios C/O and C/N allowed us to distinguish between PEG (higher C/O ratio) and chitosan (higher C/N ratio). The experimental C/O and C/N ratios for chitosan and PEG-*g*-chitosan nanoparticles are shown in Table 2. The higher C/O ratio obtained for PEG-*g*-chitosan nanoparticles is verified by the presence of PEG on the surface of nanoparticles, and a similar result was reported for chitosan/PEO-PPO nanoparticles by Calvo et al. [17]. It is likely that PEG subsequently covered the chitosan core to form the shell, since the PEG end group migrated to the surface of the nanoparticles during the preparation procedure, especially because of the hydrophilic property of PEG [18].

3.3. Characterization of PEG-g-chitosan nanoparticles

The particle sizes determined by PCS are shown in Table 3. All nanoparticles prepared by the ionotropic gelation method had sizes between 160 and 300 nm. For PE3gC64 and PE7gC64 nanoparticles, increasing the PEG molecular mass from 350 to 750 Da caused the mean particle size to increase from 218.6 to 286 nm, while increasing the PEG content from 26 to 30 wt% led to an increase of mean particle size from 166.9 to 175.3 nm for PE3gC24 and PE3gC28 nanoparticles, respectively. However, Table 3

Table 1
Materials prepared with different molar ratios of reagents

Material	PEG (Da)	Chitosan (Da)	[PEG-aldehyde]/[chitosan]	[$NaBH_4$][b]/[PEG-aldehyde]	DS[c] (%)	Graft (wt%)[d]
PE3gC64[a]	350	6000	0.4	4	17.9	26
PE3gC68	350	6000	0.8	8	24.5	32
PE7gC64	750	6000	0.4	4	9.8	29
PE7gC68	750	6000	0.8	8	20.3	46
PE3gC24	350	20,000	0.4	4	19.0	26
PE3gC28	350	20,000	0.8	8	22.0	30

[a] PE3gC64 stands for the reaction between PEG350 and chitosan (6 kDa) with the molar ratio of 0.4.
[b] Aqueous $NaBH_4$ solution.
[c] Degree of PEG substitution (DS) on monosaccharide residues of the chitosan backbone determined by elemental analysis.
[d] Graft wt% was calculated from the relation: $(W_t - W_c)/W_t \times 100\%$, where W_t is the weight of freeze-dried grafted copolymer, and W_c is the weight of chitosan.

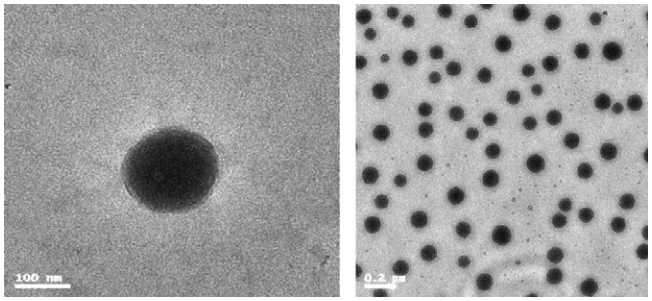

Fig. 3. TEM photographs of PEG-*g*-chitosan nanoparticles (PEG-*g*-chitosan: TPP = 5:3).

Table 2
Atomic percentage of elements on the surface of PEG-*g*-chitosan and chitosan nanoparticles

Sample	C (%)	O (%)	N (%)	C:N	C:O
PEG-*g*-chitosan nanoparticles	65.9	25.9	3.4	19.4	2.5
Chitosan nanoparticles	62.2	29.6	5.1	12.2	2.1

shows the particle size for PE3gC64 and PE3gC24 nanoparticles decreased from 218.6 to 166.9 nm when the chitosan moiety increased from 6 to 20 kDa. The increase in mean size of the PEG-*g*-chitosan nanoparticles with increasing PEG molecular mass from 350 to 750 Da was expected and could be attributed to shorter polymer chains giving rise to smaller nanoparticles. However, nanoparticles with the short-chain chitosan, PE3gC64, were unexpectedly larger than those produced from the high-chain chitosan, PE3gC24. Huang et al. [19] reported nanoparticles with a short chitosan chain (10 kDa) were unexpectedly larger than those produced from the chitosan of a molecular mass in the range 17 to 213 kDa, but the mechanism is unclear. In these cases, the smaller number of amino functional groups could have reduced the capacity of the chitosan chains for ionotropic gelation with TPP by grafting PEG onto the chitosan chain, and the resultant smaller degree of deswelling led to larger particles being produced. In addition, the size of the PE3gC28 particles (1321 nm) prepared as described by Ohya et al. [11] was much larger than that of the particles prepared by the ionotropic gelation method (175.3 nm), which was possibly caused by the preparation conditions.

The surface charge of nanoparticles was positive in the range of +16 to +30 mV (Table 3). The data show a slight decrease in zeta potential from +27.4 to +25.5 mV with increasing PEG content from 26 to 30 wt% (PE3gC24 and PE3gC28). This was attributed to the uncharged PEG "brush" coating the nanoparticle surface, which partly screened the surface charges. Furthermore, the chitosan molecular mass had a major influence on the surface charge of nanoparticles; thus, there was an increase in surface charge from +16.5 to +29.1 mV with an increase in chitosan molecular mass from 6 to 20 kDa (PE3gC64 and PE3gC24). It was noted that the zeta potential was not

Table 3
The physicochemical properties of PEG-*g*-chitosan nanoparticles

Material	Average diameters (nm)	Zeta potential (mV)[b]	Association efficiency (%)	Loading efficiency (%)	Materials/insulin (w/w)
PE3gC64	218.6 ± 2.1	16.5 ± 0.4	78.6 ± 2.4	19.5 ± 1.3	3.12:1
PE7gC64	286.5 ± 2.0	16.6 ± 0.2	85.5 ± 4.7	23.4 ± 1.9	3.12:1
PE3gC24	166.9 ± 6.6	29.1 ± 0.3	82.3 ± 3.6	20.9 ± 2.5	3.12:1
PE3gC28	175.3 ± 2.2	25.5 ± 1.2	89.8 ± 2.0	29.1 ± 0.8	3.12:1
–	–	–	90.2 ± 1.2	30.1 ± 1.9	6.25:1
–	–	–	93.5 ± 2.4	38.6 ± 2.2	12.5:1
PE3gC28	1321 ± 2.1[a]	27.4 ± 2.1	41.4 ± 3.4	9.5 ± 2.2[c]	3.12:1

Data are given as mean ± SD ($n = 3$).
[a] The particles were prepared according to the method reported by Ohya Y. et al. [11].
[b] The pH value of sample solution was 3.9.
[c] The suspension of PEG-*g*-chitosan particles was mixed with 1.0 ml of PBS (pH 8.0) containing insulin.

influenced by the two methods used for the preparation of nanoparticles in this study.

The PEG-*g*-chitosan nanoparticles displayed a high association efficiency (>78.6%) leading to insulin loading values as high as 38.6% (Table 3). These results agreed well with the previously postulated mechanism of association of insulin with chitosan nanoparticles mediated by an ionic interaction between the amino groups of chitosan and TPP. However, the low association efficacy (41.4%) of nanoparticles prepared as described by Ohya et al. was due to PEG resisting protein adsorption by the steric repulsion mechanism.

3.4. Insulin release from PEG-g-chitosan nanoparticles in vitro

The rate of insulin release from four types of nanoparticle systems was initially rapid, and then decreased after several hours (Fig. 4). This indicated that some of the insulin was adsorbed onto the surface during preparation of the nanoparticles, and then diffused rapidly when the nanoparticles came into contact with the release medium. Later, insulin was released slowly due to swelling or degradation of the polymer.

Fig. 4 shows the profiles of the cumulative release of insulin from PEG-*g*-chitosan nanoparticles with chitosan of different molecular mass (PE3gC24 and PE3gC64), and PEG content fixed at 26 wt%. The initial release of insulin from the PE3gC24 nanoparticles with 20 kDa chitosan was low. Only 16% of the trapped drug was released during the first 5 h, and about 37% in 24 h. In contrast, 70% of the insulin was released from PE3gC64 nanoparticles within the first 5 h, and about 84% in 24 h. This difference is because the PE3gC24 with 20 kDa chitosan has high positive charges, forming a tight network and effectively retarding insulin release. The higher molecular mass chitosan (20 kDa) had longer chain segments, which influenced the diffusion of insulin as well as the rate of degradation of the nanoparticles [20]. Furthermore, the rate of insulin release was affected by the PEG content; increasing the PEG content from 26 wt% (PE3gC24) to 30 wt% (PE3gC28) increased the percentage released from 16% to 19% in the first 5 h, and similar results have been reported by others [21,22]. In addition, it can be seen from Fig. 4 that the insulin release profiles from nanoparticles with PEG350 or PEG750 were different, although the chitosan molecular mass was the same (6 kDa). With PEG750, the initial burst was lower (49%) than that from the nanoparticles with PEG350 (70%), which indicated that the higher molecular mass PEG retarded insulin release. A maximum of only 84% could be released in present work, which was due to the fact that a certain amount of insulin will always stay in the formulation when equilibrium is reached after diffusion controlled release. Therefore, the release of insulin from PEG-*g*-chitosan nanoparticles was considered to be mostly by diffusion rather than the result of copolymer degradation, which is similar to the results reported by Bhattarai et al. for a PEG-*g*-chitosan hydrogel system [23].

3.5. In vivo studies

In an attempt to understand the PEG-*g*-chitosan absorption-enhancing effect, the plasma glucose levels of rabbits after intranasal administration of, a suspension of insulin-PE3gC24, a suspension of insulin-loaded PE3gC24 nanoparticles and the control insulin solution are shown in Fig. 5. Nasal administration of the control insulin solution did not reduce blood glucose level significantly (< 20% decrease) at 1 h post-administration, whereas the blood glucose level was reduced to 54% of the basal level at 1 h after administration of insulin-loaded PE3gC24 nanoparti-

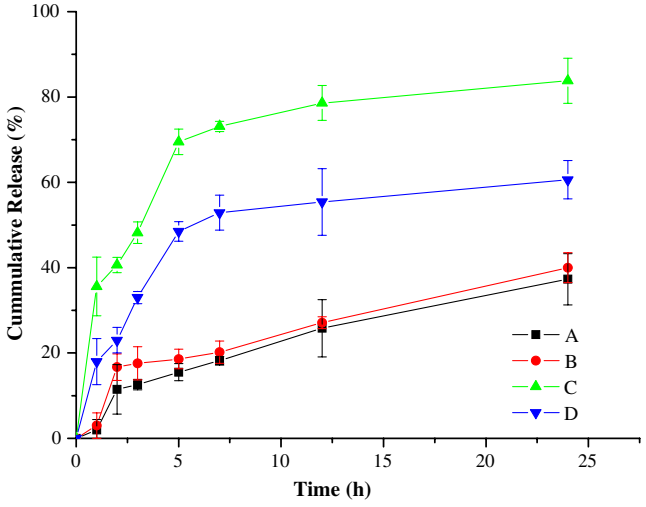

Fig. 4. *In vitro* percentage cumulative release of insulin from PEG-*g*-chitosan nanoparticles: A, PE3gC24; B, PE3gC28; C, PE3gC64; D, PE7gC64. Triplicates for each formulation were analyzed and each datum point represents the mean value ± SD ($n = 3$).

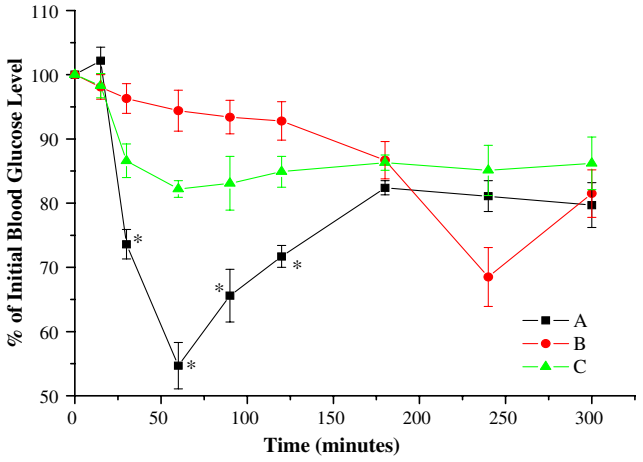

Fig. 5. Plasma glucose levels in rabbits following nasal administration (at pH 7.4) of: A, insulin-loaded PE3gC24 nanoparticles suspended in PBS; B, insulin-PE3gC24 PBS suspension; C, insulin in PBS. Mean ± SD, $n = 6$. *Statistically significant differences from control insulin solution ($p < 0.05$).

cles, and the decrease was significantly different ($p < 0.05$) from the control from 30 to 120 min after administration. The blood glucose level was 68% of baseline at 4 h post-administration of the suspension of insulin-PEG-*g*-chitosan, suggesting that PEG-*g*-chitosan can improve the systemic absorption of insulin in its active form through the nasal mucosa and that the preparation method of nanoparticles did not damage the drug.

Once the ability of PEG-*g*-chitosan nanoparticles to enhance nasal absorption of insulin was demonstrated, it was important to determine whether the composition of the PEG-*g*-chitosan affected the enhancement capacity.

Studies performed *in vivo* have shown that the PEG content has an important role in the ability to act as an absorption enhancer [24]. In order to investigate whether this effect could have a consequence *in vivo*, we compared the effects of PE3gC24 and PE3gC28 nanoparticles. Fig. 6(a) shows that PE3gC24 and PE3gC28 nanoparticles lowered blood glucose to 54% and 47% of baseline values at 60 and 120 min post-administration, respectively. The peak blood insulin levels were 203.1(±20.2) and 218.1(±33.8) μU/ml at 30 min (Fig. 6(b)), respectively. As stated above, the insulin release levels *in vitro* from nanoparticles with a high concentration of PEG were slightly higher than those with a low concentration of PEG, which is not consistent with the results reported by Wu et al. [23]. This may be because the higher concentration of PEG can prolong the circulation of PEG-*g*-chitosan nanoparticles [25]. On the other hand, the PEG-*g*-chitosan nanoparticles in this work had a core-shell structure, as shown by XPS. According to Peppas and Huang [26], after a polymer system came into contact with the mucus, the concentration gradient across the interface caused the PEG chains to diffuse out of the network and penetrated into the mucus layer. This interpenetration phenomenon was believed to increase the adhesion of PEG to the mucus. Serra et al. reported that at high PEG surface coverage the mucoadhesive capabilities of the hydrogel were considerably increased [27]. This interpenetration could be enhanced in the case of the formulation with PE3gC28, which might explain the action of PE3gC28 nanoparticles in prolonging the nasal residence time and sustaining insulin release.

We observed an effect of PEG molecular mass on the *in vivo* efficacy of PEG-*g*-chitosan nanoparticles. The lowest blood glucose levels (39% and 40% of baseline; Fig. 6(a)) occurred with PE3gC64 and PE7gC64 nanoparticles, where the blood glucose nadir occurred separately at 90 and 180 min. The plasma insulin concentrations increased rapidly, with a peak of 342.1(±26.8) and 287.3(±30.0) μU/ml at 30 min (Fig. 6(b)), respectively. The time to reach the minimum plasma glucose level was markedly delayed for PEG750 compared to PEG350. As mentioned above, as the higher molecular mass PEG was involved in this formulation, the release of insulin was retarded and the glucose concentration decreased slowly, which is consistent with the results reported by Wu et al. [24]. Moreover, Fontana et al. also observed in human

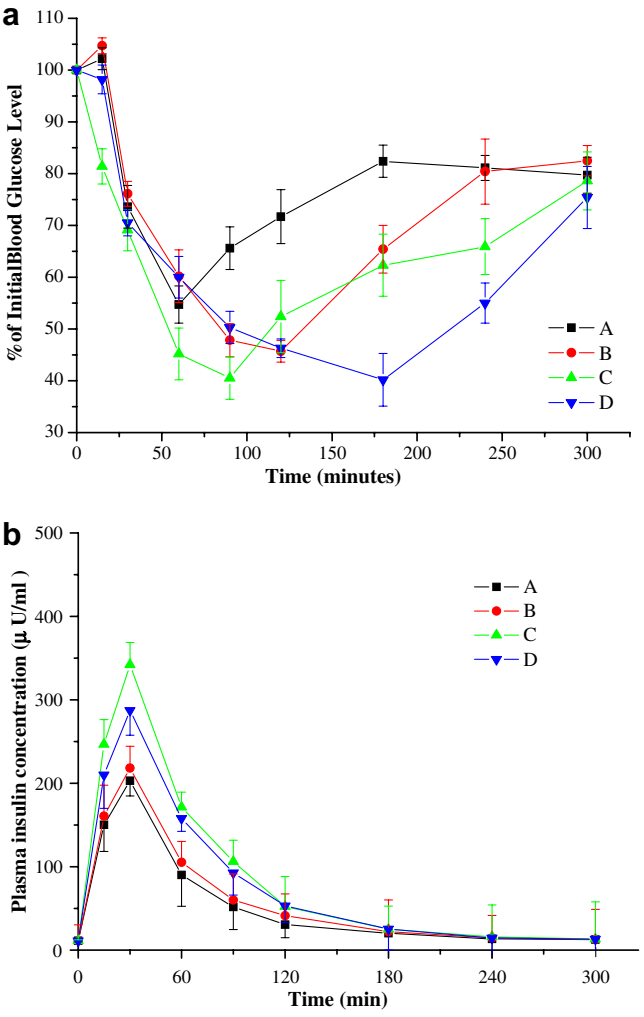

Fig. 6. *In vivo* study. (a) Plasma glucose levels in rabbits following nasal administration (at pH 7.4) of insulin-loaded PEG-*g*-chitosan nanoparticles suspended in PBS: A, PE3gC24; B, PE3gC28; C, PE3gC64; D, PE7gC64. (b) Plasma insulin concentration after administration of insulin-loaded PEG-*g*-chitosan nanoparticles: A, PE3gC24; B, PE3gC28; C, PE3gC64; D, PE7gC64. Data are the mean ± SD ($n = 6$).

plasma drug release was reduced with rising PEG molecular mass [28].

As discussed in Section 3.2, chitosan had effects on size, zeta potential and insulin loading, and on insulin release *in vivo* in the present work. As shown in Fig. 6, the nasal administration of PE3gC64 nanoparticles led to significant reduction of blood glucose levels and a rapid increase in plasma insulin concentrations compared to that obtained with PE3gC24. Moreover, the binding affinity and uptake capacity were affected by the chitosan molecular mass, which was confirmed by Huang et al. [29]. However, Vila et al. observed that the efficacy of nanoparticles on the permeability-enhancing properties was not related to the chitosan molecular mass. It is believed that this effect may vary, depending on the physiological and biological characteristics of the mucosal surface, as well as on the molecular mass, the degree of deacetylation and the form of chitosan (i.e., solution vs. particles).

Martinac et al. proposed a strong relation between zeta potential values and particle bioadhesion behavior [30]. Although slight differences in zeta potential could have an important effect in the development of non-covalent unions in the attachment process during mucoadhesion, the differences in zeta potential values seemed not to be sufficient to explain the differences in mucoadhesion behavior in the present work, where PE3gC24 nanoparticles with higher zeta potential showed a minimum blood glucose level at 30 min after nasal administration, which later returned to baseline. The effect of particle size on the extent of mucoadhesion was studied by Bravo-Osuna et al. [31], who reported that the number of nanoparticles attaching to the mucosa increased with a decrease in their hydrodynamic diameters [32]. However, according to the results of Fig. 6, the particle size is not the only factor influencing the behavior of these systems: PE3gC24 nanoparticles, with hydrodynamic diameter values around 175 nm, presented a higher blood glucose tendency in comparison with PE3gC64 nanoparticles (218 nm). It can be concluded that, for those formulations, the mucoadhesion behavior is governed by the synergistic effects of the size, zeta potential and the polymer composition.

In summary, results of *in vivo* study show that the plasma glucose levels fell sharply and remained at a low concentration for, at most, 2–3 h, and returned to baseline after 5 h. However, changes of the concentration of insulin were not the same as those of blood glucose levels, which was due to clearance of the formulations from the nasal cavity by ciliary movement. Moreover, changes in the polymeric composition could affect the mucoadhesive properties of the nanoparticles. Similarly, Wu et al. observed that HTCC-PEG-GP hydrogel prolonged the residence time of insulin in the nasal cavity [24].

4. Conclusions

PEG-*g*-chitosan nanoparticles prepared by the ionic gelation method showed an excellent capacity for association with insulin. Insulin-loaded PEG-*g*-chitosan nanoparticles displayed insulin release kinetics and properties. The molecular mass of chitosan and PEG, and DS affected *in vitro* insulin release, which yielded very interesting potential systems for drug delivery. However, chitosan molecular mass played an important role in the insulin release. Moreover, PEG-*g*-chitosan nanoparticles improved noticeably in nasal absorption of insulin compared with insulin-PEG-*g*-chitosan suspension and control insulin solution. The changes in the polymer composition clearly influenced the nasal absorption of insulin.

Acknowledgement

The starting projects for young teachers from the Ministry of Education, for financial support are gratefully acknowledged.

References

[1] Y.W. Chein, S.F. Chang, Intranasal drug delivery for systemic medications, Crit. Rev. Ther. Drug Deliv. Syst. 4 (1987) 67–194.
[2] M.A. Sarkar, Drug metabolism in the nasal mucosa, Pharm. Res. 9 (1992) 1–9.
[3] J.C. Verhoef, F.W.H.M. Merkus, Nasal absorption enhancers: relevance to drug delivery, in: A.G. Deboer (Ed.), Drug Absorption Enhancement: Concepts, Possibility, Limitations and Trends, Harwood Academic Publishers, Singapore, 1994, p. 119.
[4] K. Morimoto, M. Miyazaki, M. Kakemi, Effects of proteolytic enzyme inhibitors on nasal absorption of salmon calcitonin in rats, Int. J. Pharm. 113 (1995) 1–8.
[5] P. Dondeti, H. Zia, T.E. Needham, Bioadhesive and formulation parameters affecting nasal absorption, Int. J. Pharm. 127 (1996) 115–133.
[6] F.M.H.W. Merkus, N.G.M. Shipper, W.A.J.J. Hermens, V.S.G. Romeijin, J.C. verhoef, Absorption enhancers in nasal drug delivery: efficacy and safety, J. Control. Release 24 (1993) 201–208.
[7] L. Illum, Nasal drug delivery-possibilities, problems and solutions, J. Control. Release 87 (2003) 187–198.
[8] P. Artursson, T. Lindmark, S.S. Davis, L. Illum, Effect of chitosan on the permeability of monolayers of intestinal epithelial cells (Caco-2), Pharm. Res. 11 (1994) 1358–1361.
[9] M. Amiji, Synthesis of anionic poly(ethylene glycol)derivative for chitosan surface modification in blood-contacting applications, Carbohydr. Polym. 32 (1997) 193–199.
[10] A. Dal Pozzoa, L. Vaninia, M. Fagnonia, M. Guerrinia, A. De Benedittisb, R.A.A. Muzzarellib, Preparation and characterization of poly(ethyleneglycol)-crosslinked reacetylated chitosans, Carbohydr. Polym. 42 (2000) 201–206.
[11] Y. Ohya, R. Cai, H. Nishizawa, K. Hara, T. Ouchi, Preparation of PEG-g-chitosan nanoparticles as peptide drug carriers, S.T.P. Pharm. Sci. 10 (2000) 77–82.
[12] J.M. Harris, E.C. Struck, M.G. Case, M.S. Paley, M. Yalpani, J.M. Van Alstine, D.E. Brooks, Synthesis and characterization of poly(ethylene glycol) derivatives, J. Polym. Sci. Polym. Chem. Ed. 22 (1984) 341–352.
[13] P. Calvo, C. Remuñán-López, J.L. Vila-Jato, M.J. Alonso, Novel hydrophilic chitosan-Poly(ethylene oxide) nanoparticles as protein carriers, J. Appl. Polym. Sci. 63 (1997) 125–132.
[14] M.M. Bradford, A rapid and sensitive method for the quantitation of microgram quantities of protein utilizing the principle of protein-dye binding, Anal. Biochem. 72 (1976) 248–254.
[15] P. Dondeti, H. Zia, T.E. Needham, In vivo evaluation of spray formulations of human insulin for nasal delivery, Int. J. Pharm. 122 (1995) 91–105.
[16] S.H. Mayor, L. Illum, Investigation of the effect of anaesthesia on nasal absorption of insulin in rats, Int. J. Pharm. 149 (1997) 123–129.
[17] P. Calvo, C. Remuñán-López, J.L. Vila-Jato, M.J. Alonso, Chitosan and chitosan/ethtlene oxide-propylene oxide block copolymer nanoparticles as novel carriers for proteins and vaccines, Pharm. Res. 14 (1997) 1431–1436.
[18] T. Kaneko, K. Hamada, M.Q. Chen, M. Akashi, One-step formation of morphologically controlled nanoparticles with projection coronas, Macromolecules 37 (2004) 501–506.
[19] M. Huang, E. Khor, L.Y. Lim, Uptake and cytotoxicity of chitosan molecules and nanoparticles: effects of molecular weight and degree of deacetylation, Pharm. Res. 2 (2004) 344–353.
[20] V.R. Sinha, A.K. Singla, S. Wadhawan, R. Kaushik, R. Kumria, K. Bansal, S. Dhawan, Chitosan microspheres as a potential carrier for drugs, Int. J. Pharm. 274 (2004) 1–33.
[21] X.H. Li, X.M. Deng, Z.T. Huang, In vitro protein release and degradation of poly-DL-lactide-poly(ethylene glycol) microspheres with entrapped human serum albumin: quantitative evaluation of the factors involved in protein release phases, Pharm. Res. 18 (2001) 117–124.

[22] P. Quellec, R. Gref, E. Dellacherie, F. Sommer, M.D. Tran, M.J. Alonso, Protein encapsulation within poly(ethylene glycol)-coated nanospheres. II. Controlled release properties, J. Biomed. Mater. Res. 47 (1999) 388–395.
[23] N. Bhattarai, H.R. Ramay, J. Gunn, F.A. Matsen, M.Q. Zhang, PEG-g-chitosan as an injectable thermosensitive hydrogen for sustained protein release, J. Control. Release 103 (2005) 609–624.
[24] J. Wu, W. Wei, L.Y. Wang, Z.G. Su, G.H. Ma, A thermosensitive hydrogel based on quaternized chitosan and poly(ethylene glycol) for nasal drug delivery system, Biomaterials 28 (2007) 2220–2232.
[25] V.C. Mosqueira, P. Legrand, J.L. Morgat, M. Vert, E. Mysiakine, R. Gref, J.P. Devissaguet, G. Barratt, Biodistribution of long-circulating PEG-grafted nanoparticles in mice: effect of PEG chain length and density, Pharm. Res. 18 (2001) 1411–1419.
[26] N.A. Peppas, Y. Huang, Nanoscale technology of mucoadhesive interactions, Adv. Drug Deliv. Rev. 56 (2004) 1675–1687.
[27] L. Serra, J. Doménech, N.A. Peppas, Design of poly(ethylene glycol)-tethered copolymers as novel mucoadhesive drug delivery systems, Eur. J. Pharm. Biopharm. 63 (2006) 11–18.
[28] G. Fontana, M. Licciardi, S. Mansueto, D. Schillaci, G. Giammona, Amoxicillin-loaded polyethylcyanoacrylate nanoparticles: influence of PEG coating on the particle size, drug release rate and phagocytic uptake, Biomaterials 22 (2001) 2857–2865.
[29] M. Huang, E. Khor, L.Y. Lim, Uptake and cytotoxicity of chitosan molecules and nanoparticles: effects of molecular weight and degree of deacetylation, Pharm. Res. 21 (2004) 344–353.
[30] A. Martinac, J. Filipović-Grčić, D. Voinovich, B. Perissuti, E. Franceschinis, Development and bioadhesive properties of chitosan-ethylcellose microspheres for nasal delivery, Int. J. Pharm. 291 (2005) 69–77.
[31] I. Bravo-Osuna, C. Vauthier, A. Farabollini, G.F. Palmieri, G. Ponchel, Mucoadhesion mechanism of chitosan and thiolated chitosan-poly(isobutyl cyanoacrylate) core-shell nanoparticles, Biomaterials 28 (2007) 2233–2243.
[32] I. Bertholon, G. Ponchel, D. Labarre, P. Couvreur, C. Vauthier, Bioadhesive properties of poly(alkycyanoacrylate) nanoparticles coated with polysaccharide, J. Nanosci. Nanotechnol. 6 (2006) 3102–3109.